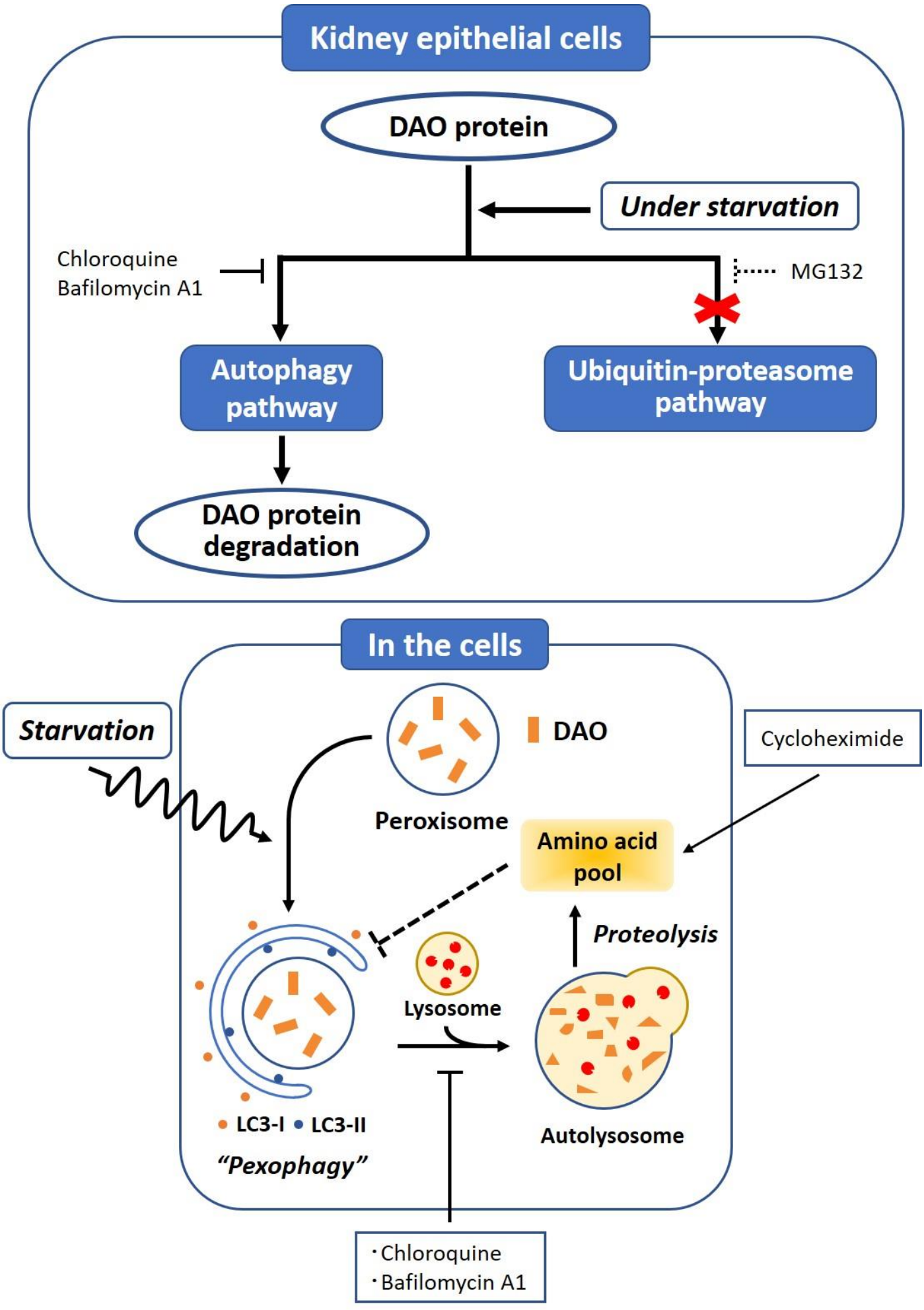
Kidney epithelial cells
DAO protein
Under starvation
Chloroquine
Bafilomycin A1
MG132
Autophagy pathway
Ubiquitin-proteasome pathway
DAO protein degradation
In the cells
Starvation
DAO
Cycloheximide
Peroxisome
Amino acid pool
Proteolysis
Lysosome
LC3-I
LC3-II
"Pexophagy"
Autolysosome
・Chloroquine
・Bafilomycin A1

Dynamics of D-amino acid oxidase in kidney epithelial cells under amino acid starvation

Hirofumi Sogabe[1], Yuji Shishido[1], Hayato Miyazaki[1], Soo Hyeon Kim[1], Wanitcha Rachadech[1,2] and Kiyoshi Fukui[1,*]

[1] Division of Enzyme Pathophysiology, Institute for Enzyme Research, Tokushima University, 3-18-15 Kuramoto, Tokushima 770-8503, Japan

[2] Division of Chemistry, Faculty of Science, Udon Thani Rajabhat University, 64 Thahan Road, Muang, Udon Thani, 41000, Thailand

Running title: Dynamics of DAO protein in kidney cells under AA starvation

*Kiyoshi Fukui, Division of Enzyme Pathophysiology, Institute for Enzyme Research, Tokushima University, 3-18-15 Kuramoto, Tokushima 770-8503, Japan. Tel: +81-88-633-7430, Fax: +81-88-633-7431, email: kiyo.fukui@tokushima-u.ac.jp

Abbreviations: AA, amino acid; AKI, acute kidney injury; ABCD3, ATP-binding cassette sub-family D member 3; CKD, chronic kidney disease; DAO, D-amino acid oxidase; DAPI, 4',6-

diamidino-2-phenylindole; EDTA, ethylenediaminetetraacetic acid; FBS, fetal bovine serum; GFR, glomerular filtration rate; HBSS, Hank's balanced salt solution; HRP, horseradish peroxidase; H_2O_2, hydrogen peroxide; IgG, immunoglobulin G; LC3, microtubule-associated protein light chain 3; PAX, paired box gene; POD, peroxidase; PMSF, phenylmethylsulfonyl fluoride; PBS, phosphate-buffered saline; Triton X-100, polyoxyethylene octyl phenyl ether; Tween 20, polyoxyethylene sorbitan monolaurate; NaCl, sodium chloride.

Abstract

D-amino acid oxidase (DAO) is a flavoenzyme catalyzing the oxidation of D-amino acid (AA)s. In the kidney, its expression is detected in proximal tubules, and DAO is considered to play a role in the conversion of D-form AAs to α-keto acids. LLC-PK_1 cells, a pig renal proximal tubule cell line, were used to elucidate the regulation of DAO protein synthesis and degradation. In this study, we showed that trypsinization of LLC-PK_1 cells in culture system rapidly reduced the intracellular DAO protein level to approximately 33.9% of that before treatment, even within 30 min. Furthermore, we observed that the DAO protein level was decreased when LLC-PK_1 cells were subjected to AA starvation. To determine the degradation pathway, we treated the cells with chloroquine and MG132. DAO degradation was found to be inhibited by chloroquine, but not by MG132 treatment. We next examined whether or not DAO was degraded by autophagy. We found that AA starvation led to an increased accumulation of LC3-II, suggesting that DAO protein is degraded by autophagy due to AA starvation conditions. Furthermore, treatment with cycloheximide inhibited DAO protein degradation. Taken together, DAO protein is degraded by autophagy under starvation. The present study revealed the potential dynamics of DAO correlated with renal pathophysiology.

Introduction

D-amino acid oxidase (DAO) is a flavoprotein that catalyzes oxidation of D-amino acid (AA)s to the corresponding imino acids and hydrogen peroxide (H_2O_2). Subsequently, the imino acid is nonenzymatically hydrolyzed to α-keto acid and ammonia (*1*). In mammals, DAO is mainly localized in the peroxisomes of cells in the kidney, liver and brain (*2, 3*). We previously reported the primary structures of porcine (*4*), human (*5*), rabbit (*6*) and mouse (*7*) kidney DAO mRNAs. In the kidney, virtually all AAs filtered by the glomerulus are returned to the plasma by absorption along the nephron (*8*). Furthermore, DAO plays an important role in not only the kidney but also the central nervous system. DAO is involved in the regulation of the brain function by metabolizing D-serine in the brain (*9*).

DAO is mainly located in peroxisomes of proximal tubular epithelial cells, where it degrades D-AAs to produce H_2O_2 (*2*). Peroxisomes have multiple functions, a major one of which is the breakdown of long-chain and very-long-chain fatty acids through β-oxidation (*10*). Another function is the degradation of active oxygen by catalase. In the methylotrophic yeast *Hansenula polymorpha*, peroxisomes are degraded by selectivity autophagy (*11*). Peroxisomes are also degraded under low-amino-acid conditions in Chinese hamster ovary cell lines (*12*). Indeed, AA starvation has been shown to induce selective peroxisome degradation (*13*). These studies suggest that the DAO and catalase activities in peroxisomes are influenced by peroxisome depletion under AA starvation conditions.

The most DAO-rich organ is the kidney in mammals, and we previously detected a 39-kDa band on Western blotting with anti-DAO antibody in LLC-PK_1 cells, which are a pig renal proximal tubule cell line (*14*). One morphological characteristic of this cell line is its dome-like structure with strong cell-cell adhesion (*15*). This line is often used in research related to DAO, but the regulation of mammalian DAO expression has not been completely clarified. We recently reported the differential regulation of DAO expression by two promoters whose activities may be modulated by the binding of paired box gene (PAX) 2 and PAX5 in LLC-PK_1 cells (*16*). This cell line has been used in studies demonstrating the important role of DAO in extracellular D-serine metabolism (*14*) and examining the efficacy of risperidone for treating schizophrenia (*17*). Therefore, we investigated the dynamics of the DAO protein level in LLC-PK_1 cells in this study.

DAO is reported to be involved in kidney disease (*18*). Acute kidney injury (AKI)-induced gut dysbiosis has been shown to contribute to the altered metabolism of D-AAs. In injured kidneys, the activity of DAO was decreased compared to that in healthy kidneys (*18*). In this study, to determine the pathophysiological role of DAO in kidney diseases, we investigated the dynamics of DAO protein.

We herein report our attempts to identify the DAO protein degradation pathway. We found that nutrition starvation induced DAO protein degradation. This process was suggested to be carried out via the autophagic pathway initiated by AA starvation.

Materials and Methods

Reagents and antibody

D-Proline, L-proline, flavin adenine dinucleotide (FAD), peroxidase (POD), sodium deoxycholate, sodium dodecyl sulphate, disodium hydrogen phosphate, potassium chloride, sodium chloride (NaCl), polyoxyethylene sorbitan monolaurate (Tween 20), phenylmethylsulfonyl fluoride (PMSF), skim milk powder and Dulbecco's Modified Eagle's Medium (high glucose) without AAs were purchased from FUJIFILM Wako Pure Chemical Corporation (Osaka, Japan). Potassium phosphate monobasic, Nonidet P-40, 4-aminoantipyrine and paraformaldehyde were obtained from Nacalai Tesque (Kyoto, Japan). *N,N*-diethyl-*m*-toluidine was purchased from TCI Chemicals (Tokyo, Japan). Polyoxyethylene octyl phenyl ether (Triton X-100) was obtained from Katayama Chemical (Osaka, Japan). Fetal bovine serum (FBS), dialyzed FBS and Medium 199 were obtained from Gibco (Carlsbad, CA, USA). Hank's balanced salt solution (HBSS), Trypsin/EDTA solution (0.25% trypsin and 0.02% ethylenediaminetetraacetic acid [EDTA]), bovine serum albumin (BSA) (Cat. No.: A7906) and mouse monoclonal anti-β-actin were purchased from Sigma-Aldrich (St. Louis, MO, USA). Anti-catalase polyclonal antibody was obtained from Proteintech (Rosemont, IL, USA). Anti-ATP-binding cassette sub-family D member 3 (ABCD3) antibody was purchased from Santa Cruz Biotechnology (Dallas, TX, USA). Anti-rabbit immunoglobulin G (IgG) and anti-mouse IgG horseradish POD (HRP)-conjugated secondary antibodies were purchased

from GE Healthcare Life Science (Little Chalfont, Bucks, UK). An Alexa Fluor 488 goat anti-rabbit IgG (H+L) highly cross-adsorbed antibody and an Alexa Fluor 555 goat anti-mouse IgG (H+L) antibody were obtained from Invitrogen (Carlsbad, CA, USA). Autophagy Watch was purchased from MBL (Nagoya, Japan) and used to determine the autophagy activity.

Cell culture

Cells from the pig renal epithelial cell line LLC-PK_1 were cultured in culture media (Medium 199 containing 5% FBS and 1% penicillin-streptomycin-glutamine solution) at 37 °C under a humidified atmosphere containing 5% CO_2. This cell line has been reported to undergo morphological changes during differentiation and maturation from subconfluent culture to a confluent epithelial layer (*17*).

AA starvation and treatment with protein degradation inhibitors

LLC-PK_1 cells were seeded at 1×10^6 cells per dish with 5 ml of culture media in a 60-mm dish for 72 h. After being washed twice with phosphate-buffered saline (PBS) (137 mM NaCl, 2.7 mM potassium chloride, 8.1 mM disodium hydrogen phosphate, 1.5 mM potassium phosphate monobasic), the cells were incubated with AA-free media (AA-free Dulbecco's Modified Eagle's Medium containing 10% dialyzed FBS) and treated with several concentrations of chloroquine (2-50 μM), MG132 (5-20 μM) or cycloheximide (0.1-50 μg/ml).

Detection of autophagy

The cultured cells were washed with PBS and then incubated for 3 h under AA starvation together with the treatment of inhibitor of autophagy (50 μM chloroquine, 100 μM bafilomycin A1 or 0.1 μg/ml cycloheximide). The amount of microtubule-associated protein light chain 3 (LC3) was detected by Autophagy Watch according to the manufacturer's instructions.

Western blot analyses

For Western blot analyses, cells were washed by PBS and collected by scraping in lysis buffer (50 mM Tris-HCl, pH 7.5, 150 mM NaCl, 1% Nonidet P-40, 1% sodium deoxycholate, 0.1% sodium dodecyl sulphate and 0.2 mM PMSF) supplemented with protease inhibitor cocktail (Roche Diagnostics, Mannheim. Germany). Cells were sonicated in a Sonifier 250 (Branson Ultrasonics Corporation, Danbury, CT, USA) followed by rotation at 4 °C for 2 h and then ultracentrifuged at 48,700 × *g* for 30 min using an Optima MAX-XP with a TLA-100.3 rotor (Beckman Coulter, Brea, CA, USA). The protein concentration was determined using a BCA kit (Pierce, Rockford, IL, USA). The cell lysates (each corresponding to 20 μg total protein) were subjected to electrophoresis on 10% (for detection of DAO, catalase, and β-actin) or 15% (for detection of LC3) polyacrylamide gels. Proteins were transferred onto an Immobilon-P Transfer Membrane (Millipore, Bedford, MA, USA). The membranes were blocked with 5%

(w/v) skim milk in washing buffer (20 mM Tris-HCl, pH 7.5, 150 mM NaCl containing 0.05% (v/v) Tween 20) and incubated with primary antibodies. A rabbit polyclonal antibody against pig DAO used for Western blotting was generated with purified DAO as an antigen (*19*). Membranes were then blocked again, and bound primary antibodies were detected by incubating with appropriate secondary antibodies conjugated with HRP. Protein bands were detected with an ECL Prime Western blotting detection reagent (GE Healthcare Life Science) according to the manufacturer's protocol and visualized with an LAS-4000 mini (FUJIFILM, Tokyo, Japan). To quantify the protein levels, the densitometry of each band was measured using the ImageJ 1.52a software program (National Institutes of Health, Bethesda, MD, USA) and normalized to β-actin. The antibodies specific to DAO (rabbit anti-DAO 1:2,000), catalase (rabbit anti-catalase 1:2,000) and β-actin (mouse anti-β-actin 1:10,000) were used. HRP-conjugated secondary antibodies (donkey anti-rabbit IgG-HRP 1:10,000; sheep anti-mouse IgG-HRP 1:20,000) were also used.

The DAO enzyme activity assay

The activity of DAO was determined by a POD-coupled colorimetric assay based on H_2O_2 production with minor modifications (*20*). Cell lysate (10 μl) was added to 96-well plates. The reaction was started by adding 90 μl of mixture (40 mM sodium phosphate buffer, pH 8.0, 16 μM FAD, 5 U/ml POD, 1.5 mM 4-aminoantipyrine, 0.23 mM *N,N*-diethyl-*m*-toluidine, 50 mM

D- or L-proline as a substrate) and incubated for 2 h at 37 °C. The absorbance of the resultant solution was measured at 545 nm using a TECAN infinite M200 plate reader (TECAN, Männedorf, Switzerland). Since the sample contained not only DAO but also a variety of enzymes, we used D-proline as a suitable substrate for DAO in consideration of its high turnover rate (*20*), and the value was calculated by subtracting the absorbance of the sample with L-proline from that with D-proline. The millimolar extinction coefficient of quinonediimine dye was 28.2 $cm^{-1}mM^{-1}$ at 545 nm.

Immunocytochemistry

$LLC\text{-}PK_1$ cells were seeded onto poly-L-lysin-coated coverslips and incubated for 72 h at 37 °C. The cells were washed in cold PBS 3 times and fixed in 4% paraformaldehyde in PBS for 30 min. The cells were permeabilized with 0.1% Triton X-100 for 3 min and blocked in blocking buffer (3% BSA in PBS) for 30 min. They were then incubated with anti-pig DAO antibodies (1:250) and anti-ABCD3 antibodies (1:500) for 1 h, followed by washing 3 times in PBS and incubation in anti-rabbit Alexa 488 (1:1,000) and anti-mouse Alexa 555 (1:1,000) for 1 h. Samples were then mounted in VECTASHIELD with 4',6-diamidino-2-phenylindole (DAPI) (Vector Laboratories, Burlingame, CA, USA), and imaged on a fluorescence microscope (BZ-X810; Keyence, Osaka, Japan).

Statistical analyses

All data in the figures show means ± standard error (SE) of the mean. Statistical analyses were performed with Student's *t*-test. Differences were considered significant if *P* values were <0.05.

Results

Trypsin/EDTA treatment promoted degradation of DAO protein in LLC-PK$_1$ cells

The pig renal proximal tubule cell line LLC-PK$_1$ has been used as an appropriate *in vitro* differentiation model for the induction of the DAO expression in renal epithelial cells. Previously, we used this cell line to identify promoter regions of the DAO gene and reported the differential regulation of the DAO expression by two promoters mediated by PAX2 and PAX5 (*15*). In addition, DAO activity was induced when a confluent monolayer was formed, accompanied by the active biosynthesis of DAO (*14*). To examine the state of intracellular biosynthesis of DAO protein after subculture, we performed Western blotting of the cell lysates. When we subcultured the cells with PBS washing twice followed by trypsin/EDTA treatment, we observed a significant reduction in the amount of DAO protein, with the level decreasing to approximately 33.9% of that before treatment (Fig. 1A, B). We observed this reduction at 30 min after seeding, and this phenomenon continued for 24 h. The DAO protein level reverted to the original level within 48 h. In addition, the DAO activity was also confirmed to be low when we measured the enzyme activity from cell lysates, as shown in Fig. 1C. We observed a significant decrease in the DAO enzyme activity at 30 min after seeding, with the level decreasing to approximately 27.8% of that before the treatment. These results indicated that trypsin/EDTA treatment promoted the degradation of DAO protein in LLC-PK$_1$ cells.

AA starvation induced the degradation of DAO protein in LLC-PK$_1$ cells

Based on the results of trypsin/EDTA treatment, we preliminarily examined the DAO protein level under various conditions, such as treatment with only trypsin, only EDTA, or other proteases (e.g. collagenase-I, dispase) instead of trypsin, all of which were dissolved in HBSS. As a result, a decrease in the DAO protein level was observed under all conditions (data not shown). Since HBSS was used as a common solvent under these conditions, LLC-PK$_1$ cells were first incubated with HBSS, which was used as a solvent for trypsin/EDTA. We observed a decrease in the DAO protein level under starved culture conditions in HBSS for 60 min, as shown in Fig. S1. HBSS represents a starvation condition, as it does not contain glucose, protein, or AAs. Based on these findings, nutrient starvation is first expected, other than the effect of detachment of cells from culture dish, to induce the degradation of DAO.

Next, we examined the effects under more restrictive conditions, such as AA starvation. We found that DAO protein was significantly decreased under AA starvation conditions at 30 min (Fig. 2A, B). Furthermore, the decrease in the DAO protein level continued until for 5 h. We found that the DAO protein level reverted to the initial level within 6 h. We also observed a similar change in the protein levels of catalase (Fig. 2A, B), which is reported to be localized in peroxisomes (*2, 21*).

We investigated the subcellular localization of DAO protein in LLC-PK$_1$ cells by immunocytochemistry and confocal imaging. As shown in Fig. 2C, we observed the co-

localization of DAO (green) and ABCD3 (red), a peroxisome marker, in LLC-PK_1 cells (yellow dots in the merged images). We found that a significant portion of DAO was colocalized with ABCD3 protein. Under AA starvation conditions, the DAO and ABCD3 signals (yellow) were decreased in the image (Fig. 2C). In addition, the DAO enzyme activity was significantly decreased under AA starvation conditions for 5 h of incubation (Fig. 2D). We also found that the DAO enzyme activity reverted to the initial level within 6 h, accompanied by an increase in the DAO protein level. Based on these results, we suspect that AA starvation induced the degradation of peroxisomal DAO protein in LLC-PK_1 cells.

The degradation of DAO protein was inhibited by chloroquine treatment instead of MG132 treatment

Next, to determine the mechanism underlying the degradation of DAO protein induced by AA starvation, we investigated the possible involvement of intracellular proteolysis in this phenomenon. We first treated LLC-PK_1 cells with chloroquine (2-50 μM) as an inhibitor of autophagy (*22*) to examine the DAO protein level under AA starvation conditions. As shown in Fig. 3A, B, chloroquine treatment inhibited the decrease in DAO protein levels during AA starvation in a dose-dependent manner. In addition, the catalase protein level also recovered following chloroquine treatment in a dose-dependent manner, and the DAO enzyme activity recovered to the control level following treatment (Fig. 3C). These results suggested that DAO

degradation was inhibited by chloroquine under AA starvation conditions.

We then examined the involvement of the ubiquitin-proteasome system under AA starvation conditions using MG132 as a proteasome inhibitor (*23*). As shown in Fig. 4A and B, the treatment of LLC-PK_1 cells with MG132 (5-20 μM) did not alter the DAO protein expression under AA starvation conditions. In addition, the levels of catalase protein and DAO enzyme activity were not influenced by MG132 treatment (Fig. 4A, C). These results indicated that MG132 has no effect on the decrease in the DAO protein level under AA starvation conditions in LLC-PK_1 cells. Given these findings, we believe that the degradation of DAO protein was mediated by the autophagy pathway instead of proteasome-dependent degradation.

Cycloheximide inhibited the degradation of DAO induced by AA starvation conditions

Inhibitors of protein synthesis, such as cycloheximide, also inhibit starvation-induced protein degradation (*24, 25*). A recent study reported that cycloheximide inhibited starvation-induced autophagy though mTORC1 (*26*). Therefore, to examine the effect of cycloheximide on the degradation of DAO protein in LLC-PK_1 cells under AA starvation conditions, the cultured cells were treated with cycloheximide (0.1-50 μg/ml). As shown in Fig. 5A, B, the degradation of both DAO and catalase proteins were inhibited after 3-h incubation with cycloheximide. Furthermore, the DAO enzyme activity was also maintained under AA starvation conditions in the presence of cycloheximide (Fig. 5C). These results suggest that DAO degradation under

AA starvation conditions was mediated by the processes in which cycloheximide interfered, indicating the involvement of the autophagy pathway or the synthesis of novel short-lived proteins essential for autophagy.

DAO degradation under AA starvation conditions was regulated by the autophagy pathway

In order to confirm the involvement of the autophagy pathway in DAO degradation under AA starvation conditions, we investigated the expression of LC3 protein, an autophagosomal marker, in LLC-PK_1 cells incubated with 50 μM chloroquine, 0.1 μg/ml cycloheximide and 100 μM bafilomycin A1, an inhibitor of autophagy. LC3 protein is present in the cytoplasm as LC3-I protein. When autophagy is induced, LC3-I is conjugated to the substrate phosphatidylethanolamine. The phosphatidylethanolamine-LC3-I conjugate is referred to as LC3-II. LC3-II is present on isolation membranes and autophagosomes and to a markedly lower degree on autolysosomes (*27*). We observed a decreasing trend in the LC3-I level and significant increase in the LC3-II level under AA starvation conditions (Fig. 6A, C, lane 2). Furthermore, the strong accumulation of LC3-II was detected by treatment with chloroquine (lane 3) and bafilomycin A1 (lane 4). In contrast, no accumulation of LC3-II was observed by treatment with cycloheximide (lane 5). These results suggest that the inhibition pathway of cycloheximide differs from those of chloroquine and bafilomycin A1. These results were consistent with the experimental data reported by a previous study on LC3 distribution under

starvation conditions (*26, 27*). It was also observed that the DAO enzyme activity was restored to the control level by the addition of bafilomycin A1 (Fig. 6D). Based on these results, we consider DAO degradation under AA starvation conditions to have been regulated by the autophagy pathway.

Discussion

In the present study, we found that the DAO protein level and DAO enzyme activity were significantly decreased under AA starvation conditions (Fig. 1S, 2). Furthermore, the DAO protein degradation and reduction of enzyme activity were inhibited by chloroquine and cycloheximide treatment (Fig. 3, 5). In contrast, MG132 treatment was unable to inhibit the DAO protein degradation or reduction of enzymatic activity (Fig. 4). In addition, we observed a significant increase in the LC3-II protein levels following both chloroquine and bafilomycin A1 treatment (Fig. 6). These results suggest that DAO protein degradation is induced by autophagy. Our findings support the fundamental understanding of DAO protein degradation in pig renal epithelial cells under AA starvation conditions.

Proteolysis plays a central role in protein renewal, which maintains the quality of proteins within cells. The two main protein degradation pathways in eukaryotic cells are the autophagy pathway and the ubiquitin-proteasome system (*28*). Cytoplasmic materials are delivered to the lysosome through various types of autophagy. Among them, macroautophagy is the major type and it has so far been analyzed most extensively. Macroautophagy is mediated by autophagosome, a unique organelle that encloses a portion of the cytoplasm for delivery to the lysosome (*29*). Our results showed that DAO and catalase proteins were decreased under AA starvation conditions (Fig. 2), and protein degradation was inhibited by chloroquine and cycloheximide (Fig. 3, 5). In addition, the LC3-II accumulation was significantly increased by

treatment with chloroquine and bafilomycin A1 (Fig. 6). The proteasome can degrade unfolded/denatured proteins (e.g. proteins damaged by oxidation) generated in response to environmental stressors in cells (*30*). In our present study, DAO protein degradation was not inhibited by MG132 (Fig. 4). Given the above findings, we hypothesized that autophagy might have caused the decreased DAO protein level in cells.

Concerning LC3-II (Fig. 6), we observed that the accumulation of LC3-II was significantly increased by treatment with chloroquine (lane 3) and bafilomycin A1 (lane 4). These results were consistent with the outcomes of previous studies on LC3-II accumulation (*27*) and suggest that autophagy was induced in LLC-PK_1 cells under AA starvation conditions. Chloroquine is a weak base and can therefore increase the pH of cellular compartments, inhibiting the activity of the degradative enzymes (*22, 31*). Bafilomycin A1, a potent and specific inhibitor of vacuolar H^+ ATPase, inhibits the acidification of lysosomes and autolysosomes. It is also reported to disturb the fusion between autophagosomes and lysosomes (*32*). Given the conditions examined in our study, chloroquine and bafilomycin A1 may have inhibited the degradation of DAO proteins by suppressing the acidification of autophagosomes.

However, LC3-II protein accumulation was not observed under cycloheximide treatment (Fig. 6, lane 5). Cycloheximide inhibits starvation-induced autophagy through the activation of mTORC1, which increases the intracellular AA pool (*26*). Rag GTPases interact with mTORC1 and activate it in response to AAs, followed by the translocation of mTORC1

to a membrane-bound compartment which contains Rheb, the mTORC1 activator (*33*). These previous findings as well as our present results concerning the degradation of DAO protein under AA starvation conditions suggest that chloroquine and bafilomycin A1 inhibit autophagy after autophagosome formation and LC3-II protein production, whereas cycloheximide inhibits autophagy before the formation of autophagosome through the activation of the mTORC1 signal.

In terms of the dynamics of DAO in LLC-PK_1 cells, we found that the DAO protein level returned to the original level within 48 h after trypsin/EDTA treatment. We tried to examine whether or not trypsin/EDTA treatment affected the promoter activity of DAO in LLC-PK_1 cells. We observed that the promoter activity was decreased by 18 h after trypsin/EDTA treatment and then gradually increased (unpublished data), suggesting that it took time for the DAO protein level to return to the original level. The mechanism underlying this phenomenon remains unclear. We also need to take various factors into consideration when performing trypsin/EDTA treatment. For example, trypsin/EDTA treatment destroys focal adhesions containing integrin, leading to a disturbance in the integrin-mediated signaling. The inhibition of focal adhesion signals in epithelial cells affects the survival and morphogenesis as well. In this context we attempted treatment with a focal adhesion kinase inhibitor in the culture media. Our preliminary results indicated that the DAO protein levels were not decreased under this condition. Therefore, we speculate that focal adhesion signals may not

have been involved in the degradation of DAO proteins. We also examined the effect of the presence of AA on trypsin/EDTA treatment and subsequent 3-hour incubation, and observed that the DAO protein levels were not decreased. However, trypsin often stimulates the protease-activated receptors in epithelial cells (*34*). Preliminary experiments using other proteases, such as collagenase-I or dispase, resulted in the degradation of DAO in LLC-PK_1 cells. As a result, it therefore remains possible that such proteases, including trypsin, may stimulate protease-activated receptors in epithelial cells (*35*). It will thus be necessary in the future to investigate the presence of protease-activated receptors and the effects of their stimulation signals on the DAO degradation in LLC-PK_1 cells. We also observed that the reduced DAO protein level and activity reverted to the original level within 6 h under AA starvation conditions. Autophagy is considered to be suppressed by the increase in the intracellular AA pool as proteolysis progresses (*26*). Therefore, it is possible that DAO protein production started within that 6-h period in LLC-PK_1 cells under AA starvation conditions, along with the concomitant suppression of autophagy.

DAO and D-serine have been reported to be involved in various diseases. Chronic kidney disease (CKD) includes a wide range of pathophysiologic processes associated with kidney dysfunction and a progressive decline in the glomerular filtration rate (GFR). Sixteen out of 21 D-AAs were detected in the plasma of patients with CKD. Among these D-AAs, D-serine was strongly associated with a poor prognosis (*36*). A previous study evaluated the

potential utility of D-serine as a GFR marker by measuring the inulin clearance and plasma D-serine simultaneously in non-CKD subjects and CKD patients (*37*). They found that the plasma levels of D-serine were interconnected with inulin clearance. This interconnection was equivalent to that observed with creatinine and cystatin C, conventional kidney disease markers. D-serine was identified as a dual marker for both the kidney function and the early detection of CKD (*37*). In addition, AKI-induced gut dysbiosis altered the metabolism of D-AAs. In AKI kidneys, the activity of DAO decreased (*18*). The blood D-serine level is regulated by the catalytic activity of DAO in the kidney, and DAO may be related to these diseases through the D-serine metabolism. However, whether or not the loss of peroxisomes plays a direct role in such kidney dysfunction still needs to be determined . Further studies will be needed in order to clarify the relationship between the loss of metabolic organelles and kidney pathogenesis under conditions of severe malnutrition.

DAO and catalase were mainly observed in the peroxisomes of cells (*2*). In our study, intracellular DAO appeared as green dots, and ABCD3 appeared as red dots on images (Fig. 2C). A similar punctate pattern of the intracellular distribution of peroxisomes was observed in transformed rat glioma cells overexpressing mouse DAO (*21*). Peroxisomes are single-membrane-bound organelles that mediate various types of metabolic reactions, such as detoxification of H_2O_2, β-oxidation of fatty acids and the biosynthesis of bile acids and ether phospholipids in mammalian cells (*2*). Peroxisomes with these diverse activities are degraded

by a selective type of autophagy known as pexophagy (*29*), which is reported to be induced under AA starvation conditions (*12*). It is possible that all peroxisomal proteins localizing in peroxisomes are degraded by pexophagy. We found that the levels of DAO protein colocalized with ABCD3 protein were decreased in cells under AA starvation conditions (Fig. 2C), whereas non-colocalizing DAO and ABCD3 proteins remained in cells after 3 h under such conditions. Given these results, it is tempting to speculate that differential pexophagy is induced in LLC-PK_1 cells under AA starvation conditions.

In conclusion, the DAO protein present in LLC-PK_1 was significantly reduced under AA starvation conditions in the present study. This decrease was caused by an autophagy-mediated pathway, not the proteasome-mediated pathway. Regardless of whether or not D-serine metabolism is linked to kidney diseases, we feel that our findings will contribute to the understanding of the importance of the DAO enzyme protein degradation pathway in kidney pathophysiology.

References

(1) Krebs, H.A. (1935) Metabolism of amino acids: deamination of amino acids. *Biochem. J.* **29**, 1620-1644

(2) De Duve, C., and Baudhuin, P. (1966) Peroxisomes (microbodies and related particles). *Physiol. Rev.* **46**, 323-357

(3) Ono, K., Shishido, Y., Park, H.K., Kawazoe, T., Iwana, S., Chung, S.P., Abou El-Magd, R.M., Yorita, K., Okano, M., Watanabe, T., Sano, N., Bando, Y., Arima, K., Sakai, T., and Fukui, K. (2009) Potential pathophysiological role of D-amino acid oxidase in schizophrenia: immunohistochemical and in situ hybridization study of the expression in human and rat brain. *J. Neural Transm.* **116**, 1335-1347

(4) Fukui, K., Watanabe, F., Shibata, T., and Miyake, Y. (1987) Molecular cloning and sequence analysis of cDNAs encoding porcine kidney D-amino acid oxidase. *Biochemistry* **26**, 3612-3618

(5) Momoi, K., Fukui, K., Watanabe, F., and Miyake, Y. (1988) Molecular cloning and sequence analysis of cDNA encoding human kidney D-amino acid oxidase. *FEBS Lett.* **238**, 180-184

(6) Momoi, K., Fukui, K., Tada, M., and Miyake, Y. (1990) Gene expression of D-amino acid oxidase in rabbit kidney. *J. Biochem*. **108**, 406-413

(7) Tada, M., Fukui, K., Momoi, K., and Miyake, Y. (1990) Cloning and expression of a

cDNA encoding mouse kidney D-amino acid oxidase. *Gene* **90**, 293-297

(8) Silbernagl, S., and Völkl, H. (1977) Amino acid reabsorption in the proximal tubule of rat kidney: stereospecificity and passive diffusion studied by continuous microperfusion. *Pflüegers Archiv*. **367**, 221-227

(9) Mothet, J.P., Parent, A.T., Wolosker, H., Brady, R.O.J., Linden, D.J., Ferris, C.D., Rogawski, M.A., and Snyder, S.H. (2000) D-serine is an endogenous ligand for the glycine site of the N-methyl-D-aspartate receptor. *Proc. Natl. Acad. Sci. USA* **97**, 4926-4931

(10) Reddy, J.K., and Hashimoto, T. (2001) Peroxisomal β-oxidation and peroxisome proliferator-activated receptor α: an adaptive metabolic system. *Annu. Rev. Nutr.* **21**, 193-230

(11) Veenhuis, M., Douma, A., Harder, W., and Osumi, M. (1983) Degradation and turnover of peroxisomes in the yeast *Hansenula polymorpha* induced by selective inactivation of peroxisomal enzymes. *Arch. Microbiol.* **134**, 193-203

(12) Hara-Kuge, S., and Fujiki, Y. (2008) The peroxin Pex14p is involved in LC3-dependent degradation of mammalian peroxisomes. *Exp. Cell Res.* **314**, 3531-3541

(13) Sargent, G., van Zutphen, T., Shatseva, T., Zhang, L., Di Giovanni, V., Bandsma, R., and Kim, P.K. (2016) PEX2 is the E3 ubiquitin ligase required for pexophagy during starvation. *J. Cell Biol.* **214**, 677-690

(14) Chung, S.P., Sogabe, K., Park, H.K., Song, Y., Ono, K., Abou El-Magd, R.M., Shishido, Y., Yorita, K., Sakai, T., and Fukui, K. (2010) Potential cytotoxic effect of hydroxypyruvate produced from D-serine by astroglial D-amino acid oxidase. *J. Biochem*. **148**, 743-753

(15) Fukui, K., Momoi, K., Watanabe, F., and Miyake, Y. (1986) Biosynthesis of porcine kidney D-amino acid oxidase. *Biochem. Biophys. Res. Commun.* **141**, 1222-1228

(16) Tran, D.H., Shishido, Y., Chung, S.P., Trinh, H.T., Yorita, K., Sakai, T., and Fukui, K. (2015) Identification of two promoters for human D-amino acid oxidase gene: implication for the differential promoter regulation mediated by PAX5/PAX2. *J. Biochem*. **157**, 377-387

(17) Abou El-Magd, R.M., Park, H.K., Kawazoe, T., Iwana, S., Ono, K., Chung, S.P., Miyano, M., Yorita, K., Sakai, T., and Fukui, K. (2010) The effect of risperidone on D-amino acid oxidase activity as a hypothesis for a novel mechanism of action in the treatment of schizophrenia. *J. Psychopharmacol*. **24**, 1055-1067

(18) Nakade, Y., Iwata, Y., Furuichi, K., Mita, M., Hamase, K., Konno, R., Miyake, T., Sakai, N., Kitajima, S., Toyama, T., Shinozaki, Y., Sagara, A., Miyagawa, T., Hara, A., Shimizu, M., Kamikawa, Y., Sato, K., Oshima, M., Yoneda-Nakagawa, S., Yamamura, Y., Kaneko, S., Miyamoto, T., Katane, M., Homma, H., Morita, H., Suda, W., Hattori, M., and Wada, T. (2018) Gut microbiota-derived D-serine protects against acute kidney

injury. *JCI Insight* **3**, e97957

(19) Fukui, K., Momoi, K., Watanabe, F., and Miyake, Y. (1988) In vivo and in vitro expression of porcine D-amino acid oxidase: in vitro system for the synthesis of a functional enzyme. *Biochemistry* **27**, 6693-6697

(20) Kim, S.H., Shishido, Y., Sogabe, H., Rachadech, W., Yorita, K., Kato, Y., and Fukui, K. (2019) Age- and gender-dependent D-amino acid oxidase activity in mouse brain and peripheral tissues: implication for aging and neurodegeneration. *J. Biochem*. **166**, 187-196

(21) Park, H.K., Shishido, Y., Ichise-Shishido, S., Kawazoe, T., Ono, K., Iwana, S., Tomita, Y., Yorita, K., Sakai, T., and Fukui, K. (2006) Potential role for astroglial D-amino acid oxidase in extracellular D-serine metabolism and cytotoxicity. *J. Biochem*. **139**, 295-304

(22) Mauthe, M., Orhon, I., Rocchi, C., Zhou, X., Luhr, M., Hijlkema, K.J., Coppes, R.P., Engedal, N., Mari, M., and Reggiori, F. (2018) Chloroquine inhibits autophagic flux by decreasing autophagosome-lysosome fusion. *Autophagy* **14**, 1435-1455

(23) Tsubuki, S., Saito, Y., Tomioka, M., Ito, H., and Kawashima, S. (1996) Differential inhibition of calpain and proteasome activities by peptidyl aldehydes of di-leucine and tri-leucine. *J. Biochem*. **119**, 572-576

(24) Kovács, A.L., and Seglen, P.O. (1981) Inhibition of hepatocytic protein degradtion by

methylaminopurines and inhibitors of protein synthesis. *Biochim. Biophys. Acta* **676**, 213-220

(25) Woodside, K.H. (1976) Effects of cycloheximide on protein degradation and gluconeogenesis in the perfused rat liver. *Biochim. Biophys. Acta* **421**, 70-79

(26) Watanabe-Asano, T., Kuma, A., and Mizushima, N. (2014) Cycloheximide inhibits starvation-induced autophagy through mTORC1 activation. *Biochem. Biophys. Res. Commun.* **445**, 334-339

(27) Mizushima, N., and Yoshimori, T. (2007) How to interpret LC3 immunoblotting. *Autophagy* **3**, 542-545

(28) Tanaka, K., and Matsuda, N. (2014) Proteostasis and neurodegeneration: the roles of proteasomal degradation and autophagy. *Biochim. Biophys. Acta* **1843**, 197-204

(29) Mizushima, N., Yoshimori, T., and Ohsumi, Y. (2011) The role of Atg proteins in autophagosome formation. *Annu. Rev. Cell Dev. Biol.* **27**, 107-132

(30) Tanaka, K., Mizushima, T., and Saeki, Y. (2012) The proteasome: molecular machinery and pathophysiological roles. *Biol. Chem.* **393**, 217-234

(31) Homewood, C.A., Warhurst, D.C., Peters, W., and Baggaley, V.C. (1972) Lysosomes, pH and the anti-malarial action of chloroquine. *Nature* **235**, 50-52

(32) Yamamoto, A., Tagawa, Y., Yoshimori, T., Moriyama, Y., Masaki, R., and Tashiro, Y. (1998) Bafilomycin A1 prevents maturation of autophagic vacuoles by inhibiting fusion

between autophagosomes and lysosomes in rat hepatoma cell line, H-4-II-E cells. *Cell Struct. Funct.* **23**, 33-42

(33) Sancak, Y., Bar-Peled, L., Zoncu, R., Markhard, A.L., Nada, S., and Sabatini, D.M. (2010) Ragulator-Rag complex targets mTORC1 to the lysosomal surface and is necessary for its activation by amino acids. *Cell* **141**, 290-303

(34) Ossovskaya, V.S., and Bunnett, N.W. (2004) Protease-activated receptors: contribution to physiology and disease. *Physiol. Rev.* **84**, 579-621

(35) Austin, K.M., Covic, L., and Kuliopulos, A. (2013) Matrix metalloproteases and PAR1 activation. *Blood* **121**, 431-439

(36) Kimura, T., Hamase, K., Miyoshi, Y., Yamamoto, R., Yasuda, K., Mita, M., Rakugi, H., Hayashi, T., and Isaka, Y. (2016) Chiral amino acid metabolomics for novel biomarker screening in the prognosis of chronic kidney disease. *Sci. Rep*. **6**, 26137

(37) Hesaka, A., Sakai, S., Hamase, K., Ikeda, T., Matsui, R., Mita, M., Horio, M., Isaka, Y., and Kimura, T. (2019) D-Serine reflects kidney function and diseases. *Sci. Rep*. **9**, 5104

Figure legends

Fig. 1. Trypsin/EDTA treatment promoted the degradation of DAO protein in LLC-PK_1 cells. LLC-PK_1 cells were incubated with culture media for 0.5-48 h after trypsin/EDTA treatment. (A) Western blotting was performed to detect DAO protein expression with anti-DAO antibody and the cytosolic marker β-actin with anti-β-actin antibody. Samples were separated by electrophoresis on 10% polyacrylamide gels. β-actin was used as a loading control. (B) The DAO protein level was quantified by densitometry. Immunoreactive bands of DAO were normalized to those of β-actin. (C) The DAO enzyme activity in the cells was measured by a colorimetric assay during the incubation period of culture after trypsin/EDTA treatment. Results represent the mean ± SE of values obtained from three independent experiments. $^{*}P < 0.05$ versus control. $^{\#}P < 0.05$ versus 0.5 h (Student's *t*-test). Cont, control.

Fig. 2. AA starvation induced the degradation of DAO and catalase in LLC-PK_1 cells. LLC-PK_1 cells were incubated with AA-free media. Catalase and ABCD3, localized proteins in peroxisomes, were also examined in comparison with DAO. (A) Cells were incubated under AA starvation conditions for 0-6 h. Western blotting was performed to detect DAO, catalase and β-actin. Samples were separated by electrophoresis on 10% polyacrylamide gels. β-actin was used as a loading control. (B) DAO and catalase protein levels were quantified by densitometry. Immunoreactive bands of DAO (open bar) and catalase (closed bar) were

normalized to those of β-actin. (C) Cells were incubated under AA starvation conditions for 0, 1 or 3 h and stained for DAO (green), ABCD3 (red) and DAPI (blue). Scale bar, 10 μm. (D) The DAO enzyme activity in the cells was measured by colorimetric assay under AA starvation conditions. Results represent the mean ± SE of values obtained from three independent experiments. $*P < 0.05$, $**P < 0.01$ and $***P < 0.005$ versus the value of DAO at 0 h. $^{\#}P < 0.05$ versus the value of catalase at 0 h (Student's *t*-test).

Fig. 3. Chloroquine inhibited the degradation of DAO and catalase under AA starvation conditions. LLC-PK_1 cells were treated with several concentrations of chloroquine for 3 h under AA starvation conditions. (A) Western blotting was performed to detect DAO, catalase and β-actin. Samples were separated by electrophoresis on 10% polyacrylamide gels. β-actin was used as a loading control. (B) DAO and catalase protein levels were quantified by densitometry. Immunoreactive bands of DAO (open bar) and catalase (closed bar) were normalized to those of β-actin. Results represent the mean ± SE of values obtained from four independent experiments. (C) The DAO enzyme activity in the cells was measured by a colorimetric assay under AA starvation conditions with chloroquine. Results represent the mean ± SE of values obtained from three independent experiments. $**P < 0.01$, $***P < 0.005$ versus the value of DAO with amino acids. $^{\#}P < 0.05$ versus the value of catalase with amino acids (Student's *t*-test).

Fig. 4. MG132 showed no effect on the decrease in the DAO and catalase protein level under AA starvation conditions. LLC-PK_1 cells were treated with several concentrations of MG132 for 3 h under AA starvation conditions. (A) Western blotting was performed to detect DAO, catalase and β-actin. Samples were separated by electrophoresis on 10% polyacrylamide gels. β-actin was used as a loading control. (B) DAO and catalase protein levels were quantified by densitometry. Immunoreactive bands of DAO (open bar) and catalase (closed bar) were normalized to those of β-actin. Results represent the mean ± SE of values obtained from four independent experiments. (C) The DAO enzyme activity in the cells was measured by colorimetric assay under AA starvation conditions with MG132. Results represent the mean ± SE of values obtained from three independent experiments. $^{*}P < 0.05$, $^{**}P < 0.01$ versus the value of DAO with amino acids. $^{\#}P < 0.05$, $^{\#\#}P < 0.01$ versus the value of catalase with amino acids (Student's *t*-test).

Fig. 5. Cycloheximide inhibited the degradation of DAO and catalase under AA starvation conditions. LLC-PK_1 cells were treated with several concentrations of cycloheximide for 3 h under AA starvation conditions. (A) Western blotting was performed to detect DAO, catalase and β-actin. Samples were separated by electrophoresis on 10% polyacrylamide gels. β-actin was used as a loading control. (B) DAO and catalase protein levels were quantified by

densitometry. Immunoreactive bands of DAO (open bar) and catalase (closed bar) were normalized to those of β-actin. Results represent the mean ± SE of values obtained from five independent experiments. (C) The DAO enzyme activity in the cells was measured by a colorimetric assay under AA starvation conditions with cycloheximide. Results represent the mean ± SE of values obtained from three independent experiments. $^{***}P < 0.005$ versus the value of DAO with amino acids. $^{\#\#}P < 0.01$ versus the value of catalase with amino acids (Student's *t*-test).

Fig. 6. AA starvation induced the accumulation of LC3-II in LLC-PK_1 cells. LLC-PK_1 cells were treated with chloroquine, bafilomycin A1 or cycloheximide for 3 h under AA starvation conditions. Lane 1, incubated with culture media; lane 2, incubated with AA-free media. To detect the accumulation of LC3-II, cells were incubated under AA starvation conditions with 50 μM chloroquine (lane 3), 100 μM bafilomycin A1 (lane 4) or 0.1 μg/ml cycloheximide (lane 5). (A) Western blotting was performed to detect DAO and β-actin. LC3-I and LC3-II proteins were detected by anti-LC3 antibody. Samples were separated by electrophoresis on 15% polyacrylamide gels. β-actin was used as a loading control. (B and C) DAO, LC3-I and LC3-II protein levels were quantified by densitometry. Immunoreactive bands of DAO (B), LC3-I (open bar) and LC3-II (closed bar) (C) were normalized to those of β-actin. Results represent the mean ± SE of values obtained from six independent experiments. (D) The DAO enzyme

activity in the cells was measured by a colorimetric assay under AA starvation conditions with or without individual reagents. Results represent the mean ± SE of values obtained from three independent experiments. *$P < 0.05$, **$P < 0.01$, ***$P < 0.005$ versus the value in the presence of amino acids (Student's *t*-test).

Funding

This work was supported in part by Japan Science and Technology Agency; CREST (Core Research for Evolutionary Science and Technology); a grant for Enzyme Research from the Japan Foundation for Applied Enzymology; H.S. is supported by the Shoshisha Foundation and the Otsuka Yoshimitu Foundation.

Acknowledgements

We thank Yusuke Kato for his valuable suggestions. We also wish to thank Kazuko Yorita for helpful comments. We thank Takanaga Ako for supporting the data collection.

Conflict of Interest

None declared.

Fig. 1

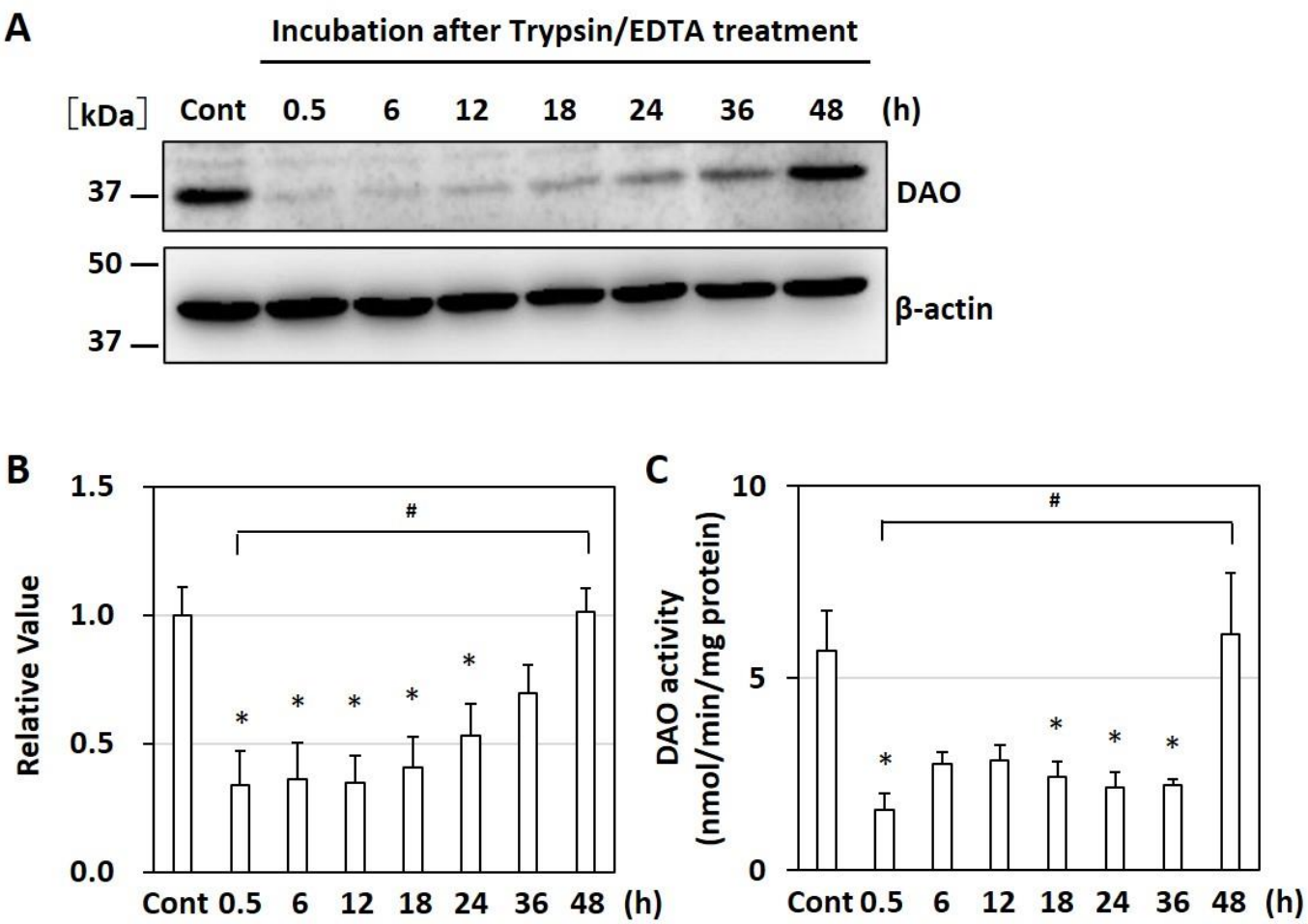
A
Incubation after Trypsin/EDTA treatment
[kDa]
Cont
0.5
6
12
18
24
36
48
(h)
37
DAO
50
37
β-actin
B
Relative Value
1.5
1.0
0.5
0.0
#
*
Cont 0.5 6 12 18 24 36 48 (h)
C
DAO activity
(nmol/min/mg protein)
10
5
0
#
*
Cont 0.5 6 12 18 24 36 48 (h)

Fig. 2

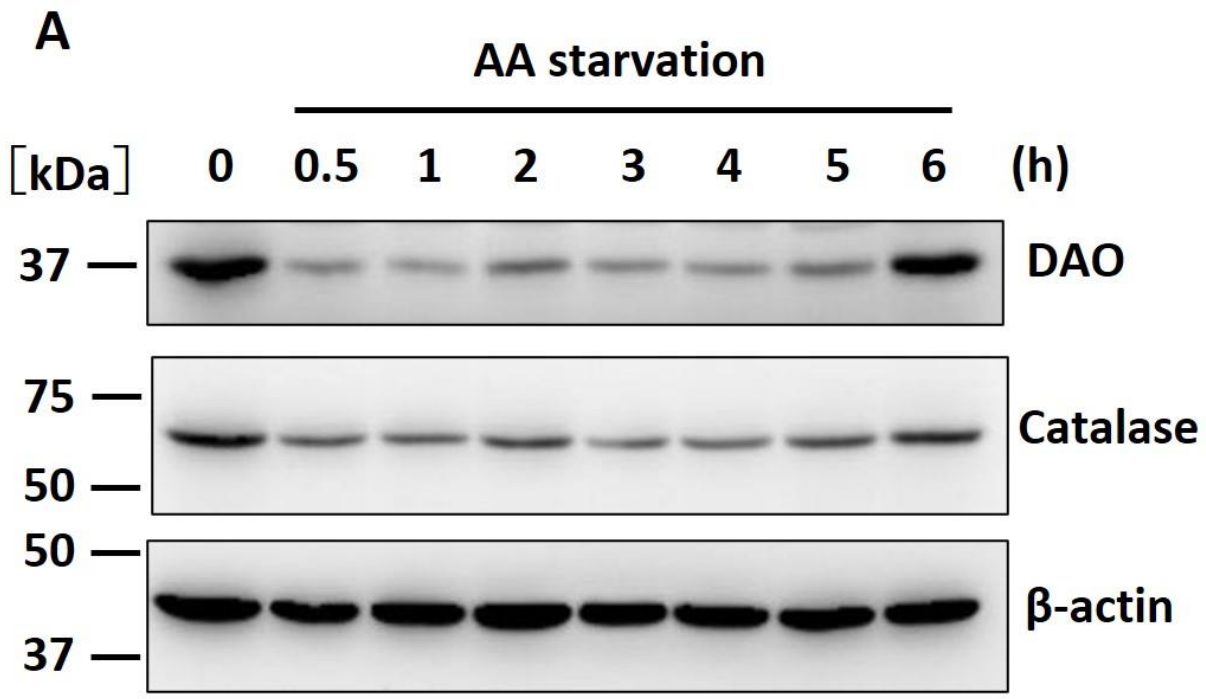
A
AA starvation
[kDa]
0
0.5
1
2
3
4
5
6
(h)
37
DAO
75
50
Catalase
50
37
β-actin

Fig. 2

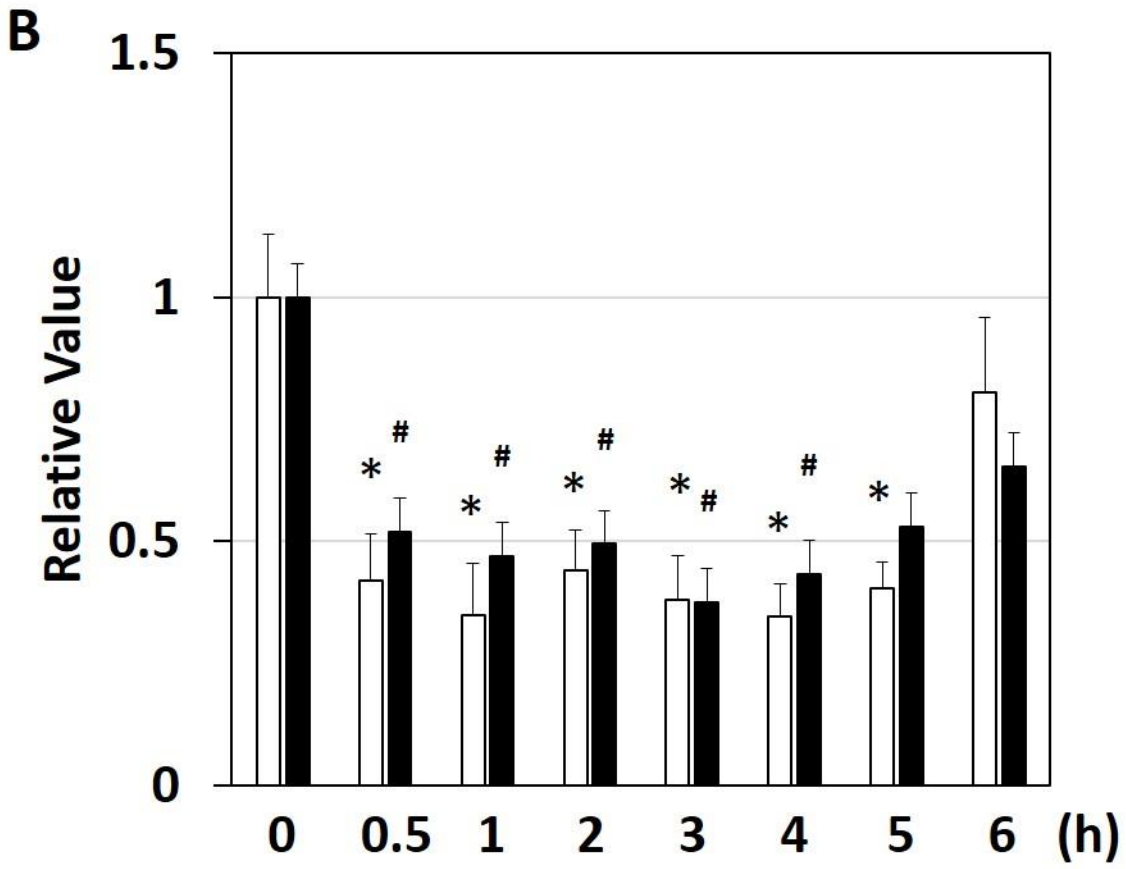

Fig. 2

C

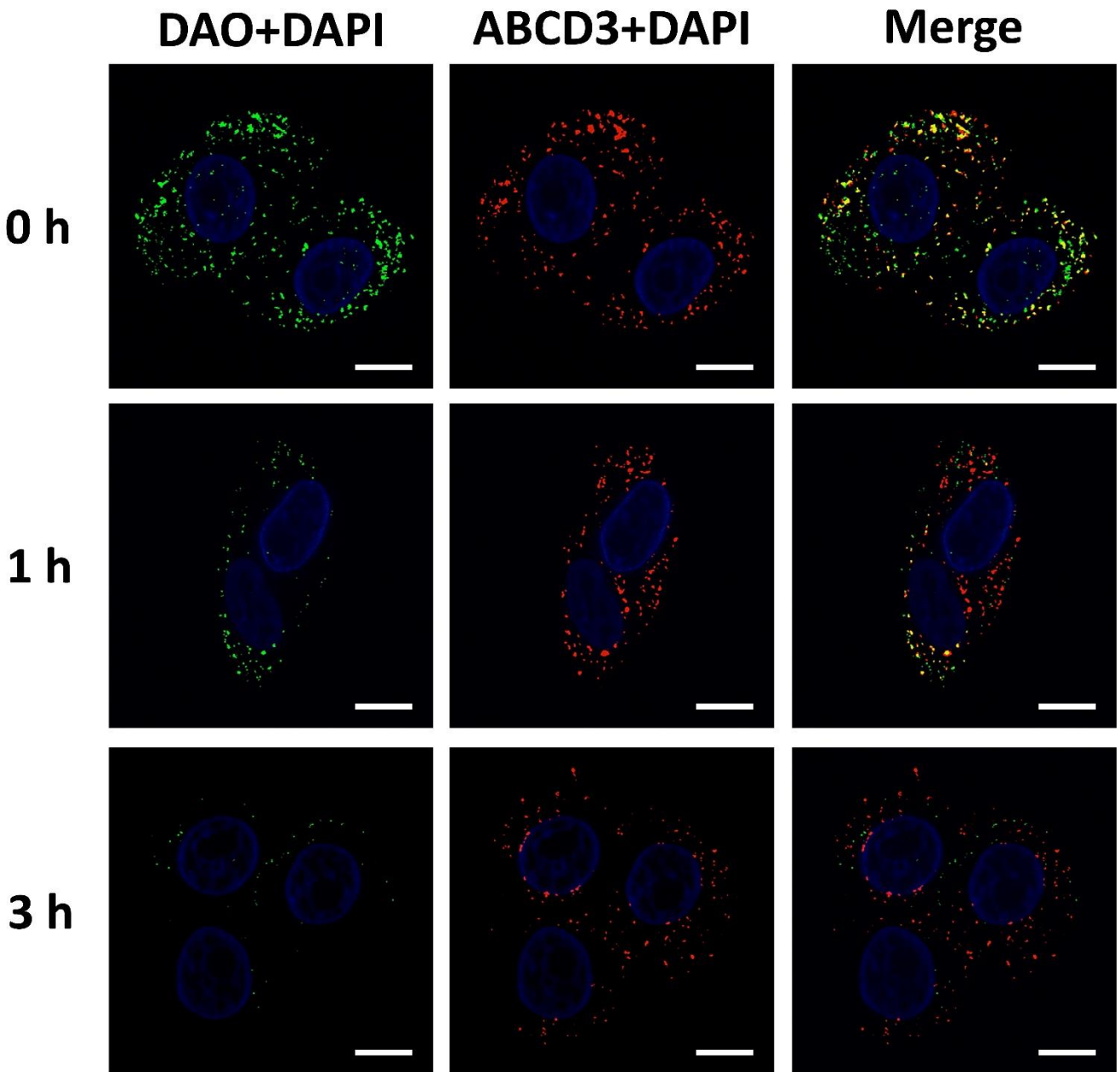

Fig. 2

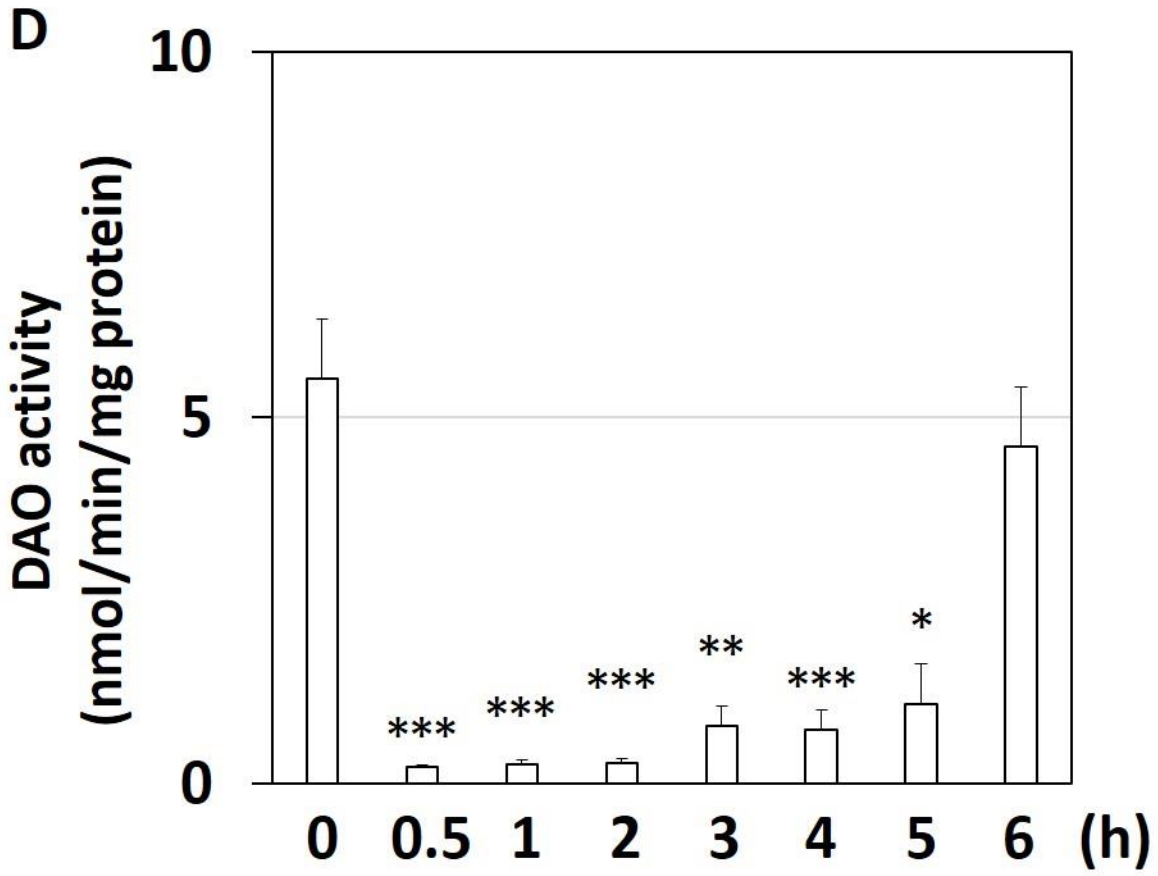

Fig. 3

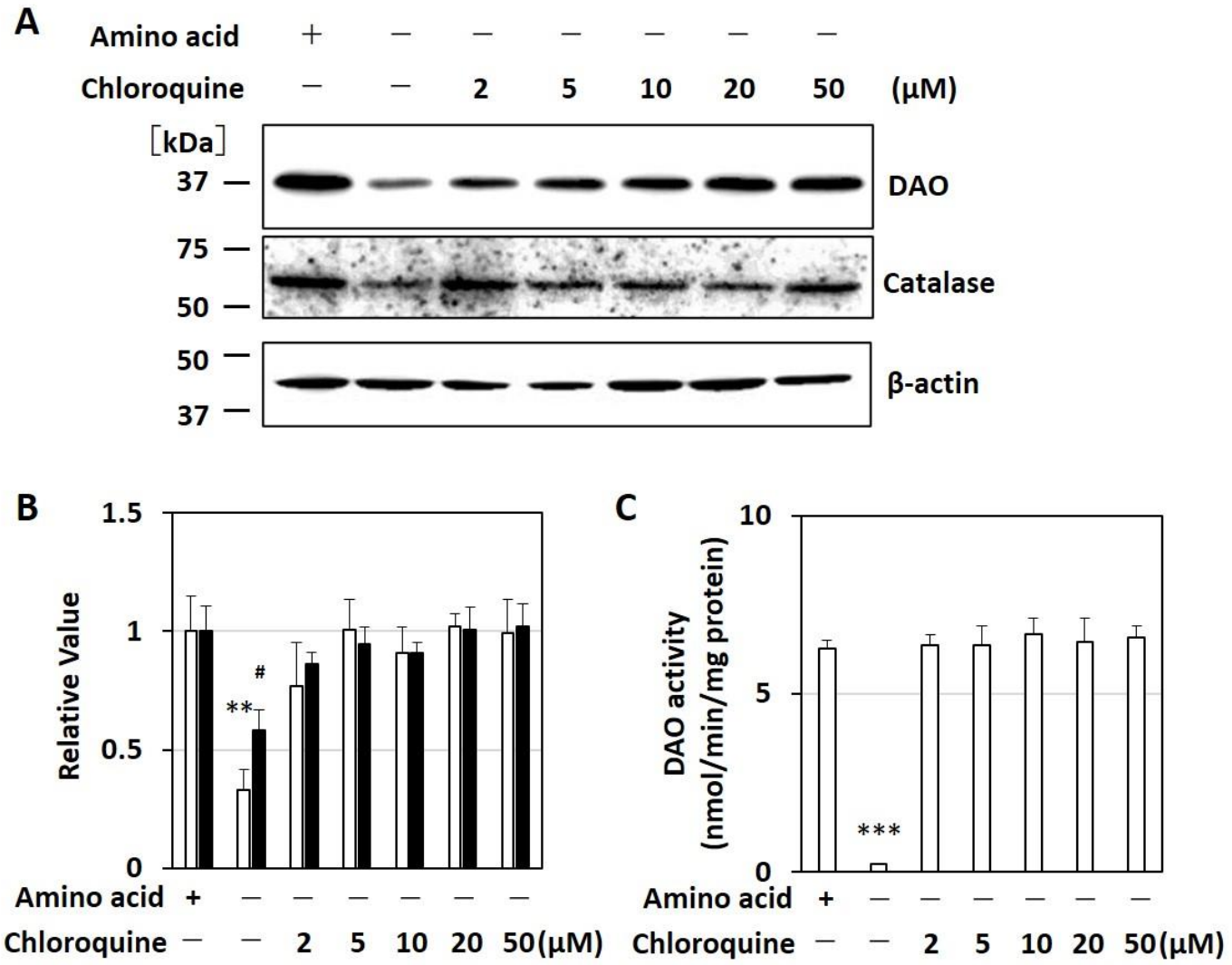
A
Amino acid + – – – – – –
Chloroquine – – 2 5 10 20 50 (μM)
[kDa]
37
DAO
75
50
Catalase
50
37
β-actin
B
Relative Value
1.5
1
0.5
0
**
#
Amino acid + – – – – – –
Chloroquine – – 2 5 10 20 50(μM)
C
DAO activity (nmol/min/mg protein)
10
5
0
***
Amino acid + – – – – – –
Chloroquine – – 2 5 10 20 50(μM)

Fig. 4

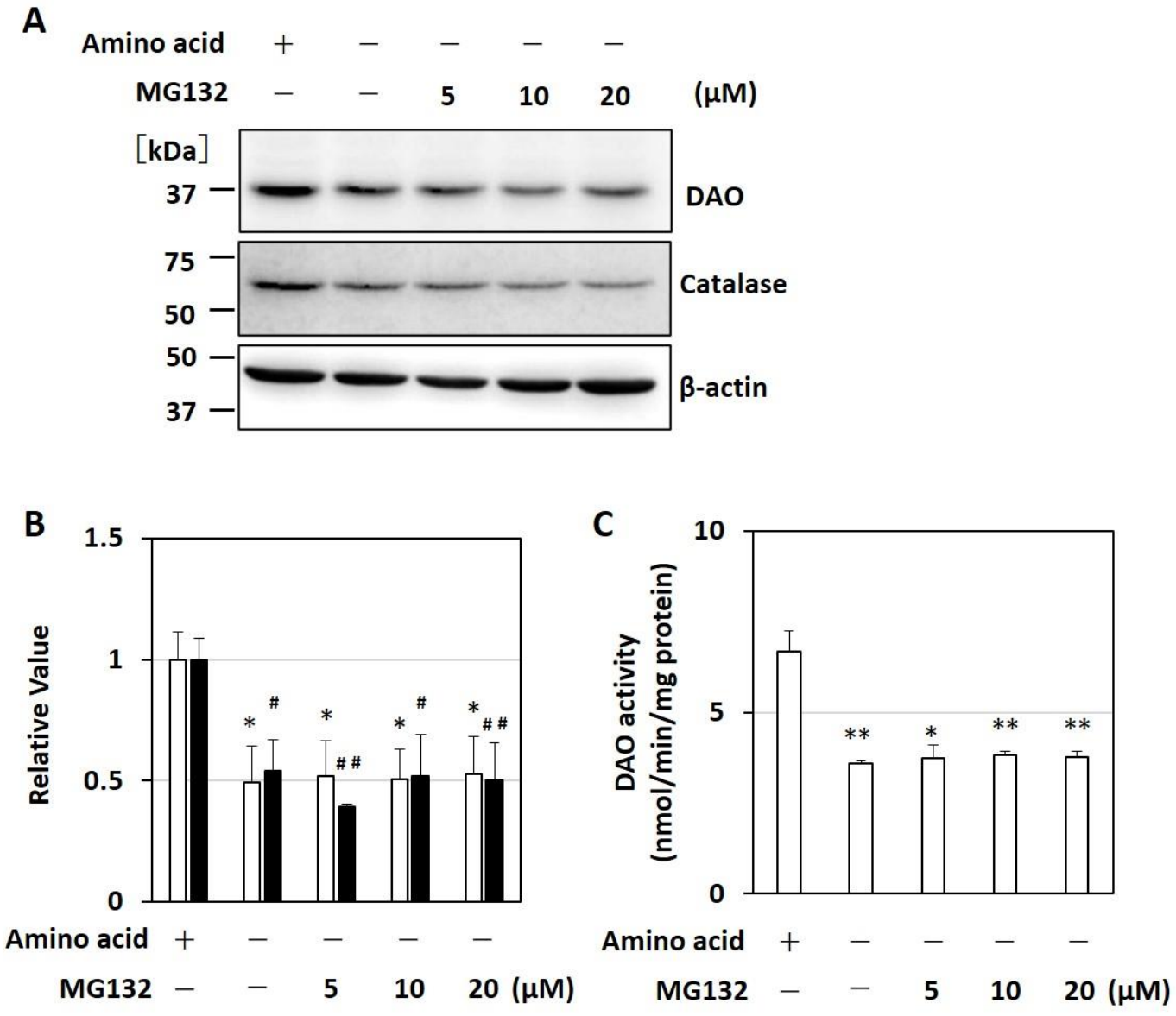
A
Amino acid + − − − −
MG132 − − 5 10 20 (μM)
[kDa]
37
DAO
75
50
Catalase
50
37
β-actin
B
Relative Value
1.5
1
0.5
0
Amino acid + − − − −
MG132 − − 5 10 20 (μM)
C
DAO activity (nmol/min/mg protein)
10
5
0
Amino acid + − − − −
MG132 − − 5 10 20 (μM)

Fig. 5

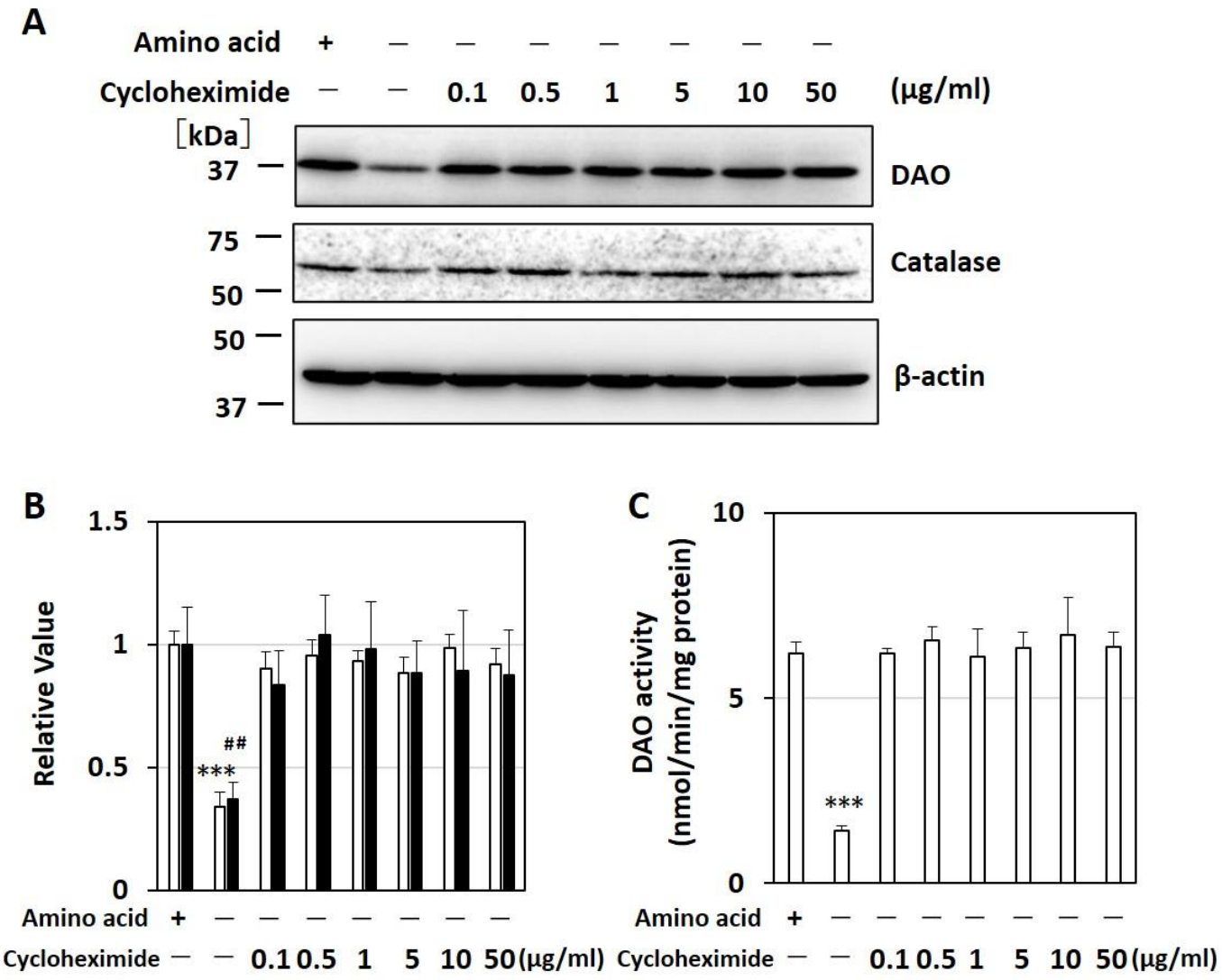
A
Amino acid + — — — — — — —
Cycloheximide — — 0.1 0.5 1 5 10 50 (μg/ml)
[kDa]
37
DAO
75
50
Catalase
50
37
β-actin
B
Relative Value
1.5
1
0.5
0
***
##
Amino acid + — — — — — — —
Cycloheximide — — 0.1 0.5 1 5 10 50 (μg/ml)
C
DAO activity (nmol/min/mg protein)
10
5
0
***
Amino acid + — — — — — — —
Cycloheximide — — 0.1 0.5 1 5 10 50 (μg/ml)

Fig. 6

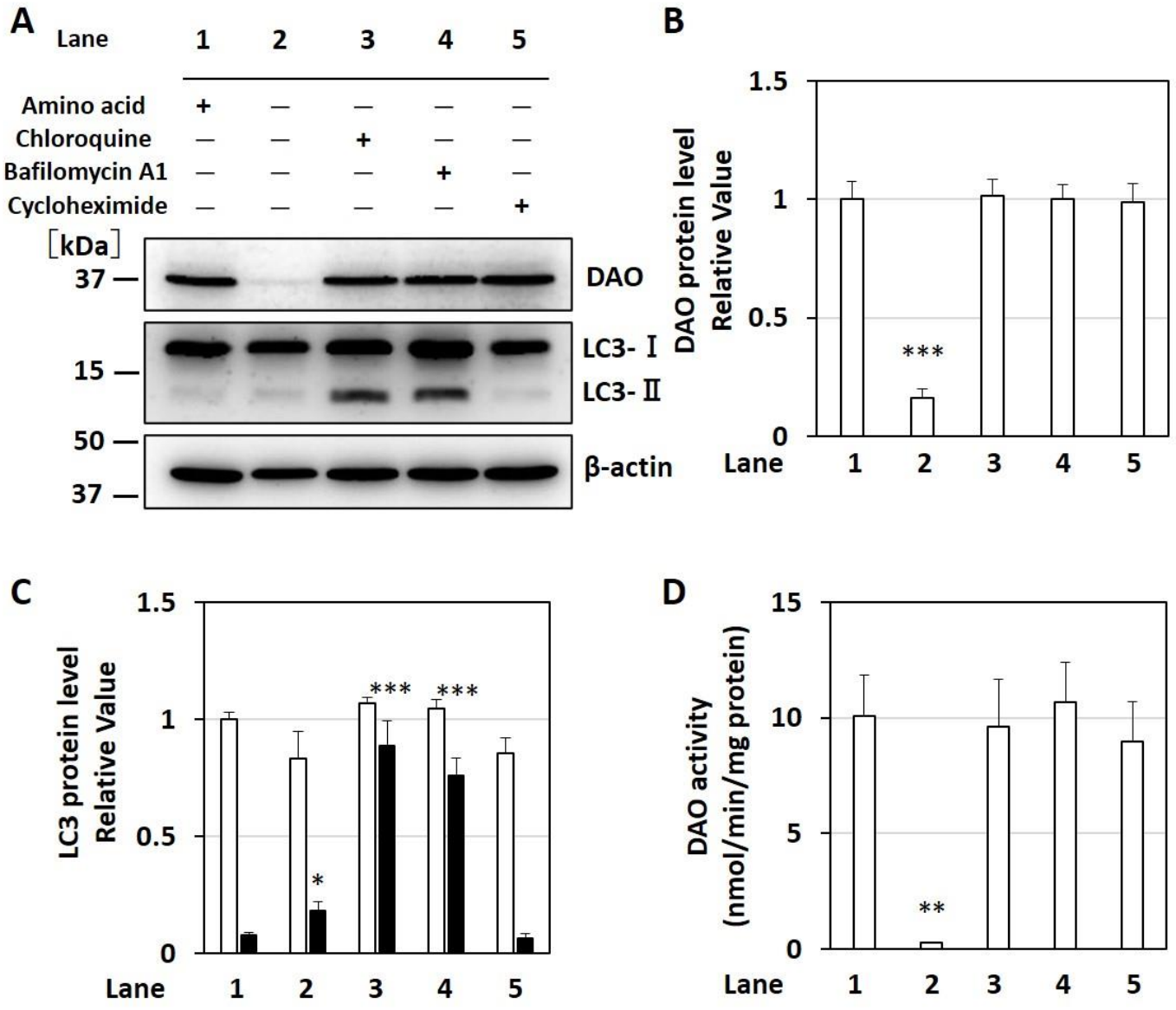
A
Lane 1 2 3 4 5
Amino acid + — — — —
Chloroquine — — + — —
Bafilomycin A1 — — — + —
Cycloheximide — — — — +
[kDa]
37
15
50
37
DAO
LC3- Ⅰ
LC3- Ⅱ
β-actin
B
DAO protein level
Relative Value
1.5
1
0.5
0
***
Lane 1 2 3 4 5
C
LC3 protein level
Relative Value
1.5
1
0.5
0
***
***
*
Lane 1 2 3 4 5
D
DAO activity
(nmol/min/mg protein)
15
10
5
0
**
Lane 1 2 3 4 5